EPJ manuscript No.
(will be inserted by the editor)

A scheme for the preparation of a polarised antineutron beam

Berthold Schoch

Physikalisches Institut, Universität Bonn, Nussallee 12, D-53115 Bonn, Germany

Received: date / Revised version: date

Abstract. A polarised antineutron beam can be prepared via electro production in the reaction $\gamma + \overline{p} \rightarrow \pi^- + \overline{n}$ by using circularly polarised virtual photons as projectils hitting a stored antiproton beam in a storage ring. High luminosities can be achieved due to the progress in cooling techniques for the antiproton beam and the development of polarised electron beams with high current, high polarisation and low emittance. In addition, multiple interaction points can be used. A tagged antineutron beam with intensities of the order of $N_{\overline{n}} = 10^3 - 10^5$ (s^{-1}) seems to be achievable. A concentration of intensity resides in the momentum range $18 \leq p_{\overline{n}}\ (GeV/c) \leq 19$ for a stored antiproton beam with a momentum of 20 GeV/c. The total momentum range is given by $14 \leq p_{\overline{n}}\ (GeV/c) \leq 19$. A cone of 7 mrad contains all produced antineutrons. A polarisation of $P_{\overline{n}} = 88\%$ of the antineutron beam can be achieved.

PACS. 13.88.+e polarisation in interactions and scattering – 29.20.Dh Storage rings – 29.27.Hj polarised beams

1 Introduction

Further progress in hadron physics depends critically on possibilities to carry out experimental programs using polarised beams and targets. In a review article [1] the authors state: "The difficulties in obtaining beams of antineutrons of suitable intensity and energy definition were overwhelming". The preparation of polarised antineutron beams is especially challenging. So far, only few experiments with unpolarised antineutrons as projectils have been carried out. At the AGS accelerator, Brookhaven, USA, an antineutron beam has been used with momenta up to 500 MeV/c [2]. An antineutron beam with momenta up to 400 MeV/c has been prepared at the CERN laboratory, Geneva, Switzerland, for experiments with the OBELIX detector [3]. Thereby, antineutron intensities of the order of $N_{\overline{n}} = 10^2/s$ at reaction target have been obtained via the charge exchange reaction p+$\overline{p}$ →n+$\overline{n}$. A tagged antineutron beam in the momentum range $5 \leq p_{\overline{n}}$ (GeV/c))$\leq$ 85 has been made available by the upgraded MIPP-spectrometer at the FERMI laboratory, Batavia, USA, providing an antineutron flux of $N_{\overline{n}} = 10^{-1}/s$ via the reaction p+$\overline{p}$ → p+π^-+$\overline{n}$ [4]. Polarised antineutron beams have not been available, so far, for physics experiments.

A method described in [5] makes use of the different absorption cross sections, $\sigma_{3/2}$ and $\sigma_{1/2}$ for the two spin projections of antiprotons stored in a storage ring interacting with circularly polarised $\gamma-$ray radiation in order to polarise antiprotons and, as a byproduct, produce polarised antineutrons. Thereby, polarised antineutrons with the same helicity will be produced by both spin projections $J_{1/2}$ and $J_{3/2}$ provided that the γ-energy stays below the two pion production threshold. In the $J_{1/2}$-channel the π^- production on the antiproton leads to a spin flip of the antineutron, in the $J_{3/2}$-channel, however, π^- production does not change the spin of the participating antinucleon. That characteristics of the reaction opens the door for a creation of an antineutron beam with high polarisation. Fig. 1 shows the cross sections $\sigma_{1/2}$ and $\sigma_{3/2}$ for the reaction γ+$\overline{p}$ $\longrightarrow$ π^- + $\overline{n}$.

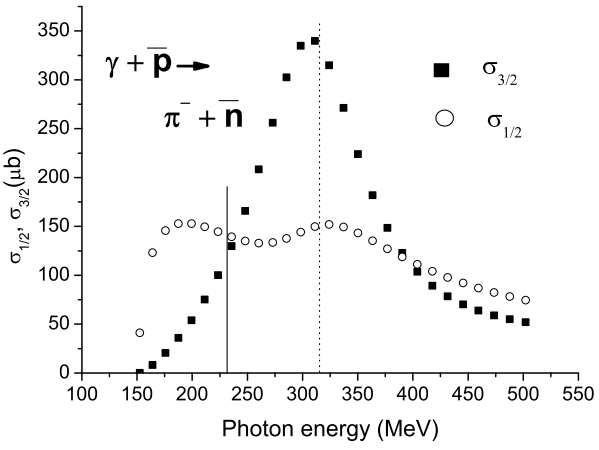

Fig. 1. The absorption cross sections $\sigma_{1/2}$ and $\sigma_{3/2}$ for γ+$\overline{p}$ $\longrightarrow$ π^- + $\overline{n}$ calculated with the MAID program [6], upper limit of integration (vertical line), two pion production threshold (dotted line)

Especially, the availability of a highly polarised antineu-

tron beam in a range of energies around 10-20 GeV and intensities of around $N_{\overline{n}} = 10^{3-5}/s$ will open up new classes of experiments in hadron physics. Together with a polarised antiproton beam complete experiments in the spin and isospin space can be performed and the time like region of the momentum transfer be explored *e.g.* with dileptons in the final state. For a possible application of the method the major question to answer will be: can a luminosity be reached to prepare a polarised antineutron beam with the intensities addressed above, preferentially, without the need of an antiproton ring with extra large acceptances.

2 Electro production versus photo production

The reactions $\gamma + \overline{p} \rightarrow \pi^- + \overline{n}$ and $\gamma + \overline{p} \rightarrow \pi^0 + \overline{p}$ can be realised by real and virtual photons. An electron beam instead of a real photon beam can be used to extract from electro induced reactions photon cross sections. Thereby, the concept of virtual photons provides the theoretical framework for that application [7]. By considering virtual photon energies close to the incoming electron energies, the so called end point region, the longitudinal contributions to the reaction cross sections are very small. By integrating over the angle $\theta_{e'}$ of the scattered electrons and applying the forward peaking approximation, $\theta_{e'} = 0$, for evaluating the response of the hadronic structure, the electro- and photo production cross sections can be related. That concept of virtual photons has been checked experimentally to an accuracy of a few percent [8]. The spectrum of virtual photons as a function of photon energy resembles, at the end point energy region, to a bremsstrahl spectrum. The intensity of virtual photons corresponds to a bremsstrahl with a radiator of the order of one percent of a radiation length. One of the big advantages by using an electron beam, compared to a γ-beam, resides in the possibility to use rather conveniently a large number of interaction points between electron and antiproton beam.

3 Ingredients determining the luminosity

The luminosity of an external electron beam interacting head on with a stored antiproton beam can be written as

$$L = N_{\overline{p}} \cdot \frac{N_e}{4\pi \cdot \sigma_x \cdot \sigma_y} \cdot \nu_c \qquad (1)$$

with the number of stored antiprotons $N_{\overline{p}}$ hitting a target of electrons of density $\frac{N_e}{4\pi \cdot \sigma_x \cdot \sigma_y}$ (electrons/cm$^2 \cdot s$) and with the frequency of the antiproton bunch of ν_c. σ_x and σ_y stand for the Gaussian beam profiles of the two intersecting beams of same extension. By choosing a virtual γ-energy range of $E_\gamma^{threshold} \leq E_\gamma \leq 230$ MeV in the rest system of the antiproton, the range of the charged pion production channel $\gamma + \overline{p} \rightarrow \pi^- + \overline{n}$ can be covered in that system as indicated in fig.1. by the vertical line as the upper limit. An electron energy of 230 MeV in the rest system of the antiproton transforms into E_e=5.39 MeV in the laboratory system by assuming an antiproton momentum in the storage ring of 20 GeV/c.

In order to use realistic numbers for the calculation of the luminosity values of beam parameters for a stored antiproton beam are taken as have been reported in the design report for the planned facility FAIR at GSI [9],[10], Darmstadt, Germany, foreseen for its High Energy Storage Ring (HESR) for the storage of antiprotons. The FAIR facility provides up to $n_{\overline{p}} = 7 \cdot 10^{10}/h$ antiprotons, thereby, the space charge limit $N_{\overline{p}}^{limit}$ for the number of stored antiprotons for a ring like HESR is $N_{\overline{p}}^{limit} \succeq 10^{13}$. Beam diameters $d_{\overline{p}}^{beam}$ at the interaction region of $d_{\overline{p}}^{beam} = 10\mu m$ can be achieved.

A tremendous progress has been made over the past fifteen years by preparing intense polarised electron beams with excellent emittances and high polarisation, see [5]. Several groups are working on a further improvement of the emittance of the beam by using *e.g.* cw guns. An increase of the current by a factor of up to 100 and an improvement of the emittance by a factor of 5-10 are envisaged in order to meet the needs for proposed Electron Ion Colliders (EIC). In addition, on the way to develop a fourth generation of synchrotron radiation sources the mode of running electron linear accelerators in an energy recovering mode has been tested successfully [11],[12]. Applications of that running mode, besides for synchrotron radiation, have not been reported so far but might be the option for the future electron antiproton interactions. With those ingredients the luminosity of the electron antiproton interactions can be calculated.

The following values are, finally, used for the calculation of the luminosity: $N_{\overline{p}}$=2 $\cdot 10^{12}$, that means a filling time of the antiproton ring of 28h, ν_c=6 $\cdot 10^5 (s_{-1})$, assuming a length of the antiproton ring of 500 m, N_e=6 $\cdot 10^{15}$, corresponding to an electron current of 1 mA and, finally, $\sigma_{x,y}$=10μm. With those values the luminosity for one interaction point (I.P.) yields by using eq. 1: $L_e^{one\ I.P.}$=9.55 $\cdot 10^{32}$ $(cm^{-2}s^{-1})$.

Depending on the lattice of the antiproton storage ring various scenarios of the e-$\overline{p}$ interaction region can be considered. The design of the lattice of the antiproton ring determines the diameter of the antiproton beam at the interaction region as well as a possible extension of that region. Such a properly chosen extension allows to implement tools like quadrupole triplets, dipols formed as wigglers or a solenoid in order to achieve more interaction points [13]. The solenoid will be chosen as an example. A beam with low energy electrons of E_e=5.39 MeV in the laboratory traversing through a solenoid with a high longitudinally magnetic field creates many foci per length. That field has almost no influence on an antiproton beam with a momentum of 20 GeV/c. With a magnetic field strength B of 10 T, *e.g.* [14], 88 foci per m can be reached. Thus many interaction points can be created on a relatively short length by implementing a strong longitudinal magnetic field. Using an interaction zone with a magnetic field strength of 10 T and an extension of 1 m a luminos-

ity of L_e=8.4 $\cdot 10^{34}$ $(cm^{-2}s^{-1})$ could be achieved. That luminosity is used to calculate reaction rates.

4 Reaction rates

With the luminosity L_e and the cross sections shown fig.1 the reaction rates for the different channels can be calculated. Each antiproton spin channel will be treated separately with a luminosity $L^{e-\overline{p}}_{1/2,3/2} = \frac{L_e}{2}$ taking into account that each channel contains half of the stored antiprotons. For each channel the reaction rates contain contributions from the unpolarized part of the virtual photon spectrum and the unpolarized part of the electron beam. The reaction rates for the two spin components of the antiprotons $N_{1/2}$ and $N_{3/2}$ as well as the rates of antineutrons N^{virt}_{unpol} and N^{unpol}_e due to the unpolarized part of the virtual photons and the unpolarized part of the electron beam, respectively, are given by

$$N = L \cdot \int_{threshold}^{E_\gamma^{\max}} x \cdot (h(E_\gamma) \cdot \frac{dN^{virtual}_\gamma(E_e)}{dE_\gamma} \cdot \sigma) dE_\gamma \quad (2)$$

with $N = N_{1/2,3/2}$, $L = L^{e-\overline{p}}_{1/2,3/2}$, $\sigma = \sigma_{1/2,3/2}$

$$N = L \cdot \int_{threshold}^{E_\gamma^{\max}} x \cdot ((1 - h(E_\gamma)) \cdot \frac{dN^{virtual}_\gamma(E_e)}{dE_\gamma} \cdot \sigma) dE_\gamma \quad (3)$$

with $N = N^{virt}_{unpol}$, $L = L_e$, $\sigma = \sigma_{tot}$

$$N^{unpol}_e = L_e \cdot \int_{threshold}^{E_\gamma^{\max}} ((1 - x) \cdot \frac{dN^{virtual}_\gamma(E_e)}{dE_\gamma} \cdot \sigma_{tot}) dE_\gamma \quad (4)$$

x stands for the degree of polarisation of the electrons. $h(E_\gamma)$ describes the helicity transfer from the electron beam to the virtual photon, see eq. 5 [5], $\frac{dN_\gamma(E_e)}{dE_\gamma}$ represents the virtual photon spectrum and $\sigma_{tot} = \sigma_{1/2} + \sigma_{3/2}$. Reaction rates are shown in table 1 for the electron energy in the rest system of the antiproton $E_e = 230MeV$ and $x = 0.85$.

$N_{1/2}$	$N_{3/2}$	N^{virt}_{unpol}	N^{unpol}_e	N^{total}_{pol}	N^{total}_{unpol}
19814	5605	2998	5040	25419	8038

Table 1 Production rates (antineutrons/s) of the different channels

The production rate of polarised antineutrons with polarised virtual photons $N_{\overline{n}}(s^{-1}) = N_{1/2} + N_{3/2}$ amounts to $N_{\overline{n}}(s^{-1})$=25419 and the total rate of unpolarised antineutrons $N^{total}_{unpol}(s^{-1}) = N^{virt}_{unpol} + N^{unpol}_e$ =8038. Half of the unpolarised antineutrons have the same helicity as the polarised antineutrons thus the polarisation of the antineutrons is given by

$$P_{\overline{n}} = \frac{N_{\overline{n}} + \frac{N^{total}_{unpol}}{2}}{N_{\overline{n}} + N^{total}_{unpol}} \quad (5)$$

and yields $P_{\overline{n}} = 88\%$ by using the rates given in table 1.

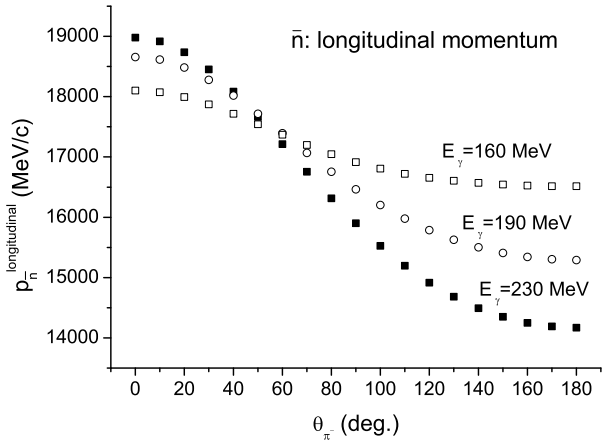

Fig. 2. Longitudinal momentum distributions of a beam of antineutrons in the laboratory system

5 Properties of the antineutron beam

Besides the overall intensity and polarisation of the antineutron beam the distribution of the longitudinal and transverse momenta are important in order to judge its possible application for future experiments. The distribution of the longitudinal momenta describes, together with the respective differential cross sections, the concentration of the strength of momenta in the extracted antineutron beam. In fig. 2 the momenta for three $\gamma-$ energies are shown, $E_\gamma = 160, 190$ and 230 MeV, as a function of the pion production angle θ_{π^-} in the rest system of the antiproton. A concentration of momenta can be seen in the momentum range 18 GeV/c $\leq p_{\overline{n}} \leq$ 19 GeV/c. This range contains a strength of around one third of the total reaction cross section for the π^- - channel. The distribution of the transverse momenta in the laboratory system determines the divergence of the beam and, thus, the range of applications in combination with suitable targets. As in fig. 2 for the longitudinal momenta, in fig. 3 the transverse momenta are shown as a function of the pion production angle θ_{π^-} for three $\gamma-$ energies in the rest system of the antiproton. The divergence of the antineutron beam is determined by the ratio $\frac{p^{transverse}_{\overline{n}}}{p^{longitudinal}_{\overline{n}}}$. A cone of 7 mrad contains all produced antineutrons. The antineutrons concentrated in the narrow momentum range 18 GeV/c $\leq p_{\overline{n}} \leq$ 19 GeV/c mentioned above show a divergence of around 5 mrad. As can be expected, the contents of fig(s) 1, 2 and 3 suggest that, provided the luminosity can be reached, the ideal running mode would be close to the pion production threshold, providing a narrow momentum range for all produced antineutrons together with a small divergence of the beam which has been one reason for choosing an electron energy of E_e=230 MeV in the rest system of the antiproton. The optimum running mode will also be influenced by the divergence of the antiproton beam in the interaction zone which might reach the same order of divergence for the final antineutron beam.

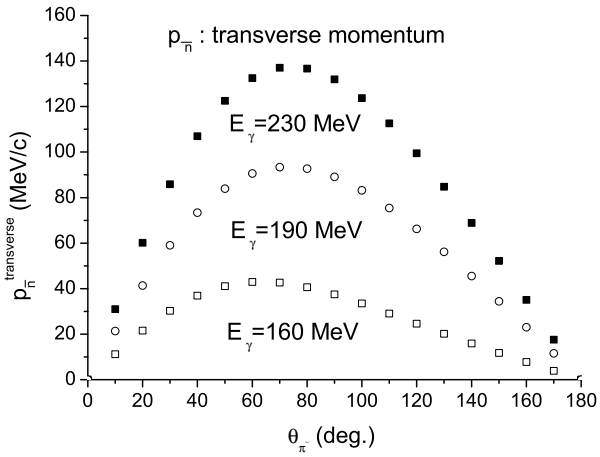

Fig. 3. Transverse momentum distributions of a beam of antineutrons in the laboratory system

The electro produced antineutrons are accompanied by negatively charged pions with momenta in the few GeV/c region and low energy electrons. Those pions and electrons can be separated from the stored antiproton beam. The detection of pion and/or electron provides a tag and thus a timing signal for antineutron induced reactions in a reaction target. Those targets, unpolarised and polarised, might be placed into the antiproton beam line by providing a hole in the middle of the target for the antiproton beam. With such a configuration luminosities up to L=$10^{28} cm^{-2} s^{-1}$ and more should become possible.

6 Losses of antiprotons

Besides the reaction process $\gamma + \overline{p} \rightarrow \pi^- + \overline{n}$ used to produce an antineutron beam two other reaction channels have to be considered, namely $\gamma + \overline{p} \rightarrow \pi^0 + \overline{p}$ and $e + \overline{p} \rightarrow e' + \overline{p}$ which might lead to losses of the stored antiproton beam. Those losses depend strongly on the momentum acceptance of the storage ring. The contribution of the $\gamma + \overline{p} \rightarrow \pi^0 + \overline{p}$ channel remains up to $E_\gamma = 230$ MeV below the rates of the $\gamma + \overline{p} \rightarrow \pi^- + \overline{n}$ channel. The $e + \overline{p} \rightarrow e' + \overline{p}$ channel, however, needs special attention. Via elastic electron scattering large momenta $\overrightarrow{q}$ can be transferred from the electron to the antiproton. The cross section σ^R for this process is given by the Rosenbluth formula [15] and decreases for low momentum transfers q at least with $\frac{1}{q^4}$ and is dominated by the transverse transfer. The rate of losses of stored antiprotons due to elastic electron scattering is given by $N_{\overline{p}}^{loss} = L_e \cdot \int_{\theta_{acc}}^{\pi} \frac{d\sigma^R}{d\Omega_{e'}} d\Omega_{e'}$. Thereby, θ_{acc} stands for the electron scattering angle determined by the momentum acceptance of the antiproton storage ring and $\frac{d\sigma^R}{d\Omega_{e'}}$ the differential cross section calculated via the Rosenbluth formula. The calculation is carried out in the rest system of the antiproton. An electron scattering angle $\theta_{acc} = 0.44(rad)$ results from the calculation by using a momentum acceptance $\frac{\Delta p}{p} = 0.005$ for the antiproton storage ring as foreseen for the HESR of the FAIR facility [9]. With the result of the integral $\int_{\theta_{acc}}^{\pi} \frac{d\sigma^R}{d\Omega_{e'}} d\Omega_{e'} = 1.87 \times 10^{-29} (cm^2)$ and the luminosity L_e the loss rate of antiprotons in the ring yields $N_{\overline{p}}^{loss} = 1.57 \times 10^6 (s^{-1})$. Thus, the loss rate due to elastic electron scattering exceeds the total number of produced antineutrons reported in sec. 4 by a factor ~ 50. This factor could be reduced in principle to ~ 1 by using an antiproton storage ring in a synchroton mode with a momentum acceptance of $\frac{\Delta p}{p} \sim 0.1$. However, as long as the loss rates of antiprotons in the storage ring are smaller than the potential fill-up rates as in the case of the FAIR project the losses can be tolerated. For the discussed case the losses are 10% of the potential maximum fill-up rate.
Electron antiproton interactions exchanging small momenta, $0 \prec \theta_e \leq \theta_{acc}$, heat up the stored antiproton beam. Thus, a cooling system must be in place for the antiproton storage ring. Cooling times of 100 - 1000 (s) as planned for the HESR ring at the FAIR facility via stochastic cooling are sufficient to provide the necessary cooling.

7 Summary

With the proposed method [5] tagged polarised antineutron beams can be prepared for the first time. Antineutron fluxes can be reached, exceeding the intensities reported so far, by choosing optimal parameter combinations in eq. 1 for the luminosity. The method can provide a wide coverage of antineutron energies by choosing suitable setups. The first test measurements for the optimization of the method will certainly use a stored proton beam. As a result a highly polarised neutron beam can be prepared via the reaction $\gamma + p \rightarrow \pi^+ + n$.

References

1. T. Bressani and A. Filippi, Phys. Rep. **383**, 213 (2003)
2. T. Armstrong *et al.*, Phys. Rev. D **36**, 659 (1987)
3. M. Agnello *et al.*, Nucl. Instr. and Meth. A **399**, 11 (1997)
4. R. Raja, arXiv:hep-ex/0701043
5. B. Schoch, EPJ A **43**, 5 (2010)
6. D. Drechsel *et al.*, Nucl. Phys. A **645**, 145 (1999)
7. R. H. Dalitz and D. R. Yennie, Phys. Rev. **105**, 1598 (1957)
8. Ch. Schmidt *et al.*, Nucl. Phys. A **392**, 345 (1983)
9. Conceptual Design Report for An International Facility for Antiproton and Ion Research. Available from http://www.gsi.de/GSI-Future/cdr
10. P. Lenisa and F. Rathmann, for PAX collaboration, arXiv:hep-ex/0505054
11. G. R. Neil *et al.*, Phys. Rev. Lett. **84**, 662 (2000)
12. CERN Courier, July/August (2010)
13. V. Kumar, Am. J. Phys. **77(8)**, August (2009) and http:/ajp.aapt.org/resource/1/ajpias/v77/i8/p737_s1
14. R. E. Laxdal *at al.*, Proceedings of LINAC 2004, Lübeck, Germany, https://accelconf.web.cern.ch/accelconf/l04/PAPERS/MOP86.PDF
15. M. N. Rosenbluth, Phys.Rev. **79**, 615 (1950)